

The Impact of Stellar Clustering on the Observed Multiplicity of Super-Earth systems: Outside-in Cascade of Orbital Misalignments Initiated by Stellar Flybys

Laetitia Rodet,^{1*} Dong Lai,¹

¹*Cornell Center for Astrophysics and Planetary Science, Department of Astronomy, Cornell University, Ithaca, NY 14853, USA*

Accepted XXX. Received YYY; in original form ZZZ

ABSTRACT

A recent study suggests that the observed multiplicity of super-Earth (SE) systems is correlated with stellar clustering: stars in high phase-space density environments have an excess of single-planet systems compared to stars in low density fields. This correlation is puzzling as stellar clustering is expected to influence mostly the outer part of planetary systems. Here we examine the possibility that stellar flybys indirectly excite the mutual inclinations of initially coplanar SEs, breaking their co-transiting geometry. We propose that flybys excite the inclinations of exterior substellar companions, which then propagate the perturbation to the inner SEs. Using analytical calculations of the secular coupling between SEs and companions, together with numerical simulations of stellar encounters, we estimate the expected number of “effective” flybys per planetary system that lead to the destruction of the SE co-transiting geometry. Our analytical results can be rescaled easily for various SE and companion properties (masses and semi-major axes) and stellar cluster parameters (density, velocity dispersion and lifetime). We show that for a given SE system, there exists an optimal companion architecture that leads to the maximum number of effective flybys; this results from the trade-off between the flyby cross section and the companion’s impact on the inner system. Subject to uncertainties in the cluster parameters, we conclude that this mechanism is inefficient if the SE system has a single exterior companion, but may play an important role in “SE + two companions” systems that were born in dense stellar clusters.

Key words: celestial mechanics – planetary systems – planet-star interactions

1 INTRODUCTION

Planets with masses/radii between Earth and Neptune, commonly called super-Earths (SEs) or mini-Neptunes, can be found around 30% of solar-type stars (e.g. [Lissauer et al. 2011](#); [Fabrycky et al. 2014](#); [Winn & Fabrycky 2015](#); [Zhu et al. 2018](#)). A large sample of them were discovered by the Kepler mission, with orbital periods below 300 days. SE systems contain an average of three planets ([Zhu et al. 2018](#)), generally “dynamically cold”, with eccentricities $e \sim 0.02$ and mutual inclinations $\Delta I \sim 2^\circ$ (e.g., [Winn & Fabrycky 2015](#)). However, there is an observed excess of single transiting planets, that could be sign of a dynamically hot sub-population of misaligned planets (so-called Kepler dichotomy, [Lissauer et al. 2011](#); [Johansen et al. 2012](#); [Read et al. 2017](#)), and indicating that the mutual inclinations in a multi-planet system decrease with the number of planets ([Zhu et al. 2018](#); [He et al. 2019](#); [Millholland et al. 2021](#)).

Recent work by [Longmore et al. \(2021\)](#) has revealed an intriguing correlation between stellar clustering and the architecture of planetary systems, in particular the multiplicity.

This work followed a similar analysis by [Winter et al. \(2020\)](#), which uncovered a correlation between stellar clustering and the occurrence of hot Jupiters. Using Gaia DR2 data ([Gaia Collaboration et al. 2018](#)), [Longmore et al. \(2021\)](#) computed the local stellar phase-space density of planet-hosting stars and their neighbours (within 40 pc) to determine whether the exoplanet host was in a relatively low or high stellar density zone compared to its neighbours. They showed that Kepler systems in local stellar phase-space overdensities have a significantly larger single-to-multiple ratio compared to those in the low phase-space density environment. The origin of this correlation is puzzling, as stellar clustering is expected to affect mostly the outer part of planetary systems in very dense environments ([Laughlin & Adams 1998](#); [Malmberg et al. 2011](#); [Parker & Quanz 2012](#); [Cai et al. 2017](#); [Li et al. 2020](#)). To account for the correlation observed by [Winter et al. \(2020\)](#), new studies have suggested that stellar flybys excite the eccentricities and inclinations of outer planets/companions, which then trigger the formation of hot Jupiters from cold Jupiters via high-eccentricity migration ([Wang et al. 2020](#); [Rodet et al. 2021](#)). For this flyby scenario to be effective, certain requirements (derived analytically in [Rodet et al. 2021](#)) on the companion property (mass and

* E-mail: lbr63@cornell.edu

semi-major axis) and the cluster property (such as stellar density and age) must be satisfied. In this paper, we will examine a similar “outside-in” effect of stellar flybys on the SEs systems.

In recent years, long-period giant planets have been observed in an increasing number of SE systems. Statistical analysis combining radial velocity and transit observations suggests that, depending on the metallicities of their host stars, 30–60 % of inner SE systems have cold Jupiter companions (Zhu & Wu 2018; Bryan et al. 2020). The dynamical perturbations from external companions can excite the eccentricities and mutual inclinations of SEs, thereby influencing the observability (co-transiting geometry) and stability of the inner system (Boué & Fabrycky 2014; Carrera et al. 2016; Lai & Pu 2017; Huang et al. 2017; Mustill et al. 2017; Hansen 2017; Becker & Adams 2017; Read et al. 2017; Pu & Lai 2018; Denham et al. 2019; Pu & Lai 2020; Rodet & Lai 2021). This requires the giant planets to be dynamically hot, which can be achieved by planet-planet scattering. Alternatively, in dense stellar environments, the eccentricities and inclinations of giant planets can be induced by stellar flybys.

In this paper, we examine the possibility that SEs systems become misaligned following a stellar encounter (“flyby-induced misalignment cascade” scenario), using a combination of analytical calculations (for the secular planet interactions) and numerical simulations (for stellar flybys). In Section 2, we outline the proposed scenario and its key ingredients. In Section 3, we examine the inclination requirement for an outer companion to break the co-transiting geometry of two inner initially coplanar SEs. In Section 4, we evaluate the extent to which a stellar encounter can raise the inclination of an outer companion. In Section 5, we derive the expected number of “effective” flybys (i.e. those that succeed in breaking the co-transiting geometry of SEs) per system as a function of the properties of the planetary system (SEs+companion) and its stellar cluster environment. Finally, in Section 6, we extend our calculation to SE systems with two outer companions. In Section 7, we summarize our main results, recalling the key figures and equations of the paper.

2 SCENARIO: FLYBY-INDUCED MISALIGNMENT CASCADE

The observed excess of single-transiting SEs or mini-Neptunes could be sign of a dynamically hot sub-population of inner ($\lesssim 0.5$ au) planets with appreciable mutual inclinations. The recently-evidenced correlation between single-transiting systems and stellar clustering suggests that stellar environments could play a significant role in this misalignment. However, close-in SEs are largely protected from perturbations induced by the stellar environment thanks to their proximity to the host star.

According to recent statistical estimates, 30–60% of inner SE systems have cold Jupiter companions ($\gtrsim 1$ au, mass $\gtrsim 0.3 M_J$; see Zhu & Wu 2018; Bryan et al. 2020). Such companions widen the effective cross section of the planetary system, and thus its vulnerability to the dynamical perturbations from the stellar environment. The architecture of the inner SEs can be indirectly impacted by stellar flybys through the eccentricity/inclination excitations of the outer companions.

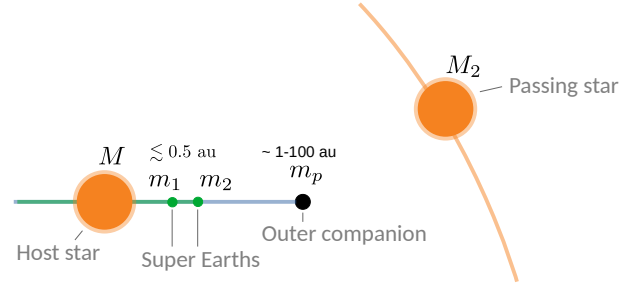


Figure 1. Schematic of the flyby-induced misalignment cascade scenario: An initially coplanar system comprising two inner planets (SEs) and an outer companion encounters a passing star. The stellar flyby changes the orbital inclination of m_p , which then induces misalignment between the orbits of m_1 and m_2 .

In this paper, we consider a system of two SEs with masses m_1, m_2 and semimajor axes $a_1 < a_2 \lesssim 0.5$ au, on circular coplanar orbits around a host star (mass $M = M_1 \sim 1 M_\odot$, radius $R_1 \sim 1 R_\odot$). An outer companion (mass $m_p \ll M$) is located at a_p on an initially circular coplanar orbit (see Figure 1). In Section 6 we will consider the case of two exterior companions surrounding SEs.

The system may experience close encounters with other stars, if the stellar density is large enough. This is typically the case in the beginning of the planetary system’s life, when it is embedded in its dense birth cluster. Most of these clusters are loosely bound or unbound, so that they tend to be disrupted over tens of millions of years. However, in the early phase of the cluster, close encounters may be frequent enough to influence the planetary architecture.

We denote e_p and I_p the eccentricity and inclination of the companion m_p after an encounter with a passing star M_2 . The inclined companion then induces mutual inclination within the SEs through secular interactions. In order for the SEs to break their co-transiting geometry, their relative inclination ΔI must be greater than a critical value

$$\Delta I_{\text{crit}} \simeq \frac{R_1}{a_2} \simeq 0.5^\circ \left(\frac{a_2}{0.5 \text{ au}} \right)^{-1} \left(\frac{R_1}{1 R_\odot} \right). \quad (1)$$

In the following sections, we will derive the minimum required inclination of the companion $I_{p,\text{crit}}$ to break the SEs co-transiting geometry, and the corresponding likelihood that a stellar encounter would generate such an inclination.

3 SECULAR DYNAMICS OF PLANET MISALIGNMENT

When the outer companion planet to the SEs in an initially coplanar system suddenly becomes misaligned by I_p , the mutual inclination ΔI between the SEs will oscillate around a forced value (Lai & Pu 2017; Rodet & Lai 2021). In the following, we derive the minimum misalignment $I_{p,\text{crit}}$ required for the forced inclination to be greater than the critical value ΔI_{crit} (see equation 1). In theory however, due to the oscillation of ΔI , the co-transiting geometry of the SEs will be broken only part of the time even if the forced inclination is greater than ΔI_{crit} .

The forced mutual inclination ΔI of the SEs depends on I_p , m_p and a_p , as well as on mutual coupling between the inner planets. Denote ω_{ik} the characteristic nodal precession frequency of planet i induced by the gravitational torque from planet k . The frequencies of mutual interactions in the inner two planets are

$$\omega_{12} = \frac{\omega_{21} L_2}{L_1} = \frac{1}{4} n_1 \frac{m_2}{M} \left(\frac{a_1}{a_2} \right)^2 b_{\frac{3}{2}}^{(1)} \left(\frac{a_1}{a_2} \right), \quad (2)$$

while the precession frequencies of the SEs induced by the companion are

$$\omega_{1p} \equiv \frac{1}{4} n_1 \frac{m_p}{M} \left(\frac{a_1}{a_p} \right)^2 b_{\frac{3}{2}}^{(1)} \left(\frac{a_1}{a_p} \right), \quad (3)$$

$$\omega_{2p} \equiv \frac{1}{4} n_2 \frac{m_p}{M} \left(\frac{a_2}{a_p} \right)^2 b_{\frac{3}{2}}^{(1)} \left(\frac{a_2}{a_p} \right), \quad (4)$$

[see Eq. (7.11) in Murray & Dermott (2000)]. Here $n_i = \sqrt{GM/a_i^3}$ and $L_i = m_i \sqrt{GM a_i}$ are the mean motion and the orbital angular momentum of planet i , and $b_s^{(j)}(\alpha)$ is the Laplace coefficient:

$$b_s^{(j)}(\alpha) = \frac{1}{\pi} \int_0^{2\pi} \frac{\cos(jx) dx}{(1 - 2\alpha \cos x + \alpha^2)^s}, \quad (5)$$

with $b_{\frac{3}{2}}^{(1)}(\alpha) \simeq 3\alpha(1 + 15\alpha^2/8 + 175\alpha^4/64 + \dots)$ for $\alpha \ll 1$. When the two SEs are away from any mean-motion resonances (see Rodet & Lai 2021), the forced misalignment ΔI between them induced by the inclined companion m_p depends on the coupling parameter $\varepsilon_{12,p}$ (Lai & Pu 2017), given by

$$\varepsilon_{12,p} = \frac{\omega_{2p} - \omega_{1p}}{\omega_{12} + \omega_{21}} \equiv \varepsilon_{12} \frac{\tilde{m}_p}{\tilde{a}_p^3}, \quad (6)$$

where we have defined $\tilde{m}_p \equiv m_p/(1 M_J)$ and $\tilde{a}_p \equiv a_p/(1 \text{ au})$. When $a_1, a_2 \ll a_p$ and $m_p \ll M$, ε_{12} is independent of a_p and m_p :

$$\varepsilon_{12} \simeq \frac{1 M_J}{m_2} \left(\frac{a_2}{1 \text{ au}} \right)^3 \hat{\varepsilon}_{12}, \quad (7)$$

where

$$\hat{\varepsilon}_{12} = \frac{3a_1/a_2}{b_{3/2}^{(1)}(a_1/a_2)} \frac{(a_2/a_1)^{\frac{3}{2}} - 1}{1 + L_1/L_2}. \quad (8)$$

The accuracy of equation (7) is better than 10% for $a_p > 5a_2$. Note that $\hat{\varepsilon}_{12}$ does not depend on the semimajor axis and mass scales of the SE system, and depends only on a_2/a_1 and m_1/m_2 . The variation of $\hat{\varepsilon}_{12}$ with a_2/a_1 is shown in Figure 2, for different values of m_2/m_1 .

We can now write down the forced misalignment ΔI of the two SEs as a function of the companion's inclination I_p and the coupling parameter $\varepsilon_{12,p}$. We identify two regimes: strong coupling, where $\varepsilon_{12,p} \lesssim 1$, and weak coupling, where $\varepsilon_{12,p} \gtrsim 1$. In the strong coupling regime, the companion's influence is weaker than the coupling between the SEs, and the forced inclination is proportional to $\varepsilon_{12,p}$:

$$\Delta I \simeq \frac{1}{2} \sin(2I_p) \varepsilon_{12,p}, \quad (\text{for } \varepsilon_{12,p} \lesssim 1). \quad (9)$$

On the other hand, in the weak coupling regime, the coupling between the SEs is negligible and the forced inclination reaches

$$\Delta I \simeq I_p, \quad (\text{for } \varepsilon_{12,p} \gtrsim 1). \quad (10)$$

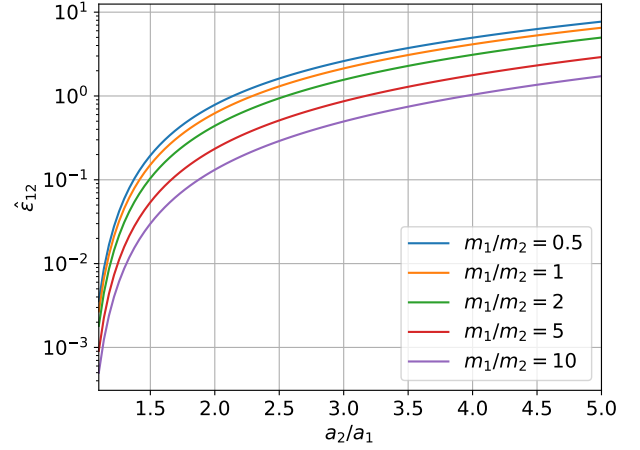


Figure 2. The rescaled coupling parameter $\hat{\varepsilon}_{12}$ as a function of the semimajor axis ratio a_2/a_1 of the SE system, for different mass ratios m_1/m_2 (see equation 8). Systems with higher $\hat{\varepsilon}_{12}$ are more easily perturbed by the outer companion.

In the intermediate regime, ΔI transitions smoothly from equation (9) to equation (10). There is an exception: when $m_1 \ll m_2$, the misalignment between the SEs can become very high (larger than I_p) as $\varepsilon_{12,p}$ approaches 1 (Lai & Pu 2017). In this paper, we ignore this resonant case and assume $m_1 \gtrsim m_2$, so that equations (9)–(10) provide adequate description for the forced misalignment.

Using equations (6)–(10), we can derive $I_{p,\text{crit}}$ (that gives $\Delta I = \Delta I_{\text{crit}}$) as a function of the rescaled semi-major axis of the companion $\tilde{a}_p/\tilde{m}_p^{1/3}$ for a given ε_{12} . In the weak coupling regime,

$$\varepsilon_{12,p} \gtrsim 1 \iff \tilde{a}_p/\tilde{m}_p^{1/3} \lesssim \varepsilon_{12}^{1/3}, \quad (11)$$

we have

$$I_{p,\text{crit}} \simeq \Delta I_{\text{crit}}, \quad (12)$$

i.e. when the outer companion is close to the inner SE system, the required inclination only needs to be as low as ΔI_{crit} . In the strong coupling regime,

$$\varepsilon_{12,p} \lesssim 1 \iff \tilde{a}_p/\tilde{m}_p^{1/3} \gtrsim \varepsilon_{12}^{1/3}, \quad (13)$$

we have

$$\begin{aligned} I_{p,\text{crit}} &\simeq \frac{1}{2} \arcsin \left(\frac{2\Delta I_{\text{crit}}}{\varepsilon_{12,p}} \right) \\ &= \frac{1}{2} \arcsin \left(\frac{2\Delta I_{\text{crit}} \tilde{a}_p^3}{\varepsilon_{12} \tilde{m}_p} \right), \end{aligned} \quad (14)$$

i.e. when the outer companion is far from the SEs, the required inclination increases with a_p . The argument of the arcsin cannot be more than 1; it follows that for given ε_{12} and \tilde{m}_p , there is a maximum possible \tilde{a}_p for the companion, above which it cannot possibly induce a misalignment ΔI_{crit} , regardless of the value of I_p . This maximum is set by $\Delta I_{\text{crit}} = \varepsilon_{12,p}/2$, giving

$$\begin{aligned} \tilde{a}_{p,\text{max}} &= \left(\frac{\varepsilon_{12} \tilde{m}_p}{2\Delta I_{\text{crit}}} \right)^{\frac{1}{3}} \\ &\simeq 3.9 \varepsilon_{12}^{\frac{1}{3}} \tilde{m}_p^{\frac{1}{3}} \left(\frac{\Delta I_{\text{crit}}}{0.5^\circ} \right)^{-\frac{1}{3}}. \end{aligned} \quad (15)$$

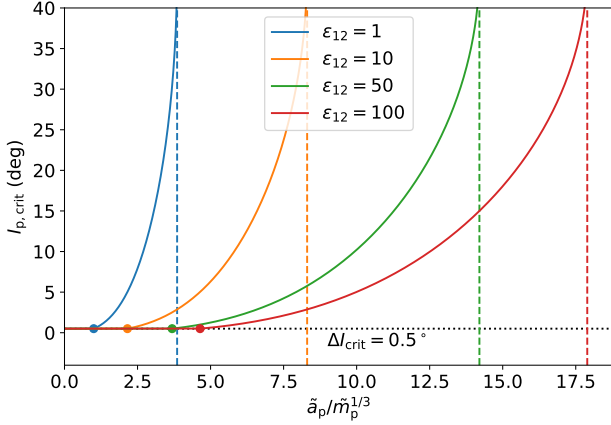


Figure 3. Minimum companion’s inclination $I_{p,\text{crit}}$ required to produce a forced misalignment $\Delta I_{\text{crit}} = 0.5^\circ$ between two SEs (equations 12,14), as a function of the scaled companion semi-major axis, $\tilde{a}_p/\tilde{m}_p^{1/3} = a_p/(1 \text{ au}) (m_p/M_J)^{-1/3}$, for different inner SEs systems, characterized by different values of ε_{12} (see equation 7). The horizontal dashed line indicates $\Delta I_{\text{crit}} = 0.5^\circ$, the filled circles indicate the change of regimes (between $\varepsilon_{12,p} > 1$ and $\varepsilon_{12,p} < 1$), while the vertical dashed lines indicate the maximum $\tilde{a}_p/\tilde{m}_p^{1/3}$, beyond which it is impossible to generate $\Delta I_{\text{crit}} = 0.5^\circ$ regardless of the I_p value (see equation 15).

Figure 3 shows the critical I_p required to produce $\Delta I_{\text{crit}} = 0.5^\circ$ as a function of $\tilde{a}_p/\tilde{m}_p^{1/3}$, for different SE systems (characterized by different values of ε_{12}). In the next section, we will derive the likelihood for a flyby to excite the companion’s inclination from 0 to $I_p > I_{p,\text{crit}}$.

4 EFFECT OF FLYBY ON THE OUTER PLANET

In this section, we calculate the expected effect of a stellar flyby on the orbit of the outer planet/companion, and estimate the likelihood that the companion can attain $I_p > I_{p,\text{crit}}$. To this end, we perform a suite of N -body simulations to determine the distribution of the post-flyby inclination I_p and eccentricity e_p . Following the similar approach as in Rodet et al. (2021), we suppose that the companion (with $m_p \ll M_2$, the mass of the flyby star) is on an initially circular orbit, and we ignore the inner planets (their proximity to the host star effectively shields them from stellar encounter). We integrate a nearly-parabolic ($e = 1.1$) encounter between two equal-mass stars using IAS15 from the REBOUND package. The integration time is chosen so that the distance between M_1 and M_2 is equal to $100a_p$ at the beginning and end of each simulation, and the time-step is adaptive. We sample uniformly the dimensionless distance at closest approach $\tilde{q} \equiv q/a_p$ (where q is the periastron of the encounter) from 0.05 to 10, the cosine of the inclination $\cos i$, and the argument of periastron ω of the flyby, and the initial phase λ_p of the planet m_p . For each \tilde{q} , we carry out $30 \times 20 \times 20$ (in $\cos i, \omega, \lambda_p$) = 12,000 simulations, and obtain the final orbital elements of the planet.

4.1 Effect on the inclination

For a given \tilde{q} , we derive $p(e_p < 1)$, the probability that the planet remains bound, and $p(I_p > I_{p,\text{min}})$, the probability that the planet remains bound and has a final inclination larger than $I_{p,\text{min}}$. These probabilities are shown in Figure 4 as a function of \tilde{q} , for different values of $I_{p,\text{min}}$. For $\tilde{q} \gtrsim 3$, $p(I_p > I_{p,\text{min}})$ can be derived analytically using the secular approach. This derivation is detailed in the Appendix, as well as the comparison with the N -body results.

Using our result for $p(I_p > I_{p,\text{min}})$, we can derive the number of flybys that successfully raise the inclination of the outer planet (at a_p) above certain $I_{p,\text{min}}$. This number can be written as a product of a scaling factor and a geometric function (Rodet et al. 2021):

$$\mathcal{N}(I_p > I_{p,\text{min}}, a_p) = \mathcal{N}_{\text{close}}(a_p) \times f(I_{p,\text{min}}), \quad (16)$$

where $\mathcal{N}_{\text{close}}(a_p)$ is the number of fly-by with $q < a_p$. Assuming that gravitational focusing is dominant in the close encounter and that the velocities of stars in the cluster follow the Maxwell-Boltzmann distribution, we have (Rodet et al. 2021)

$$\begin{aligned} \mathcal{N}_{\text{close}}(a_p) &= \frac{2\sqrt{2}\pi a_p G M_{\text{tot}} n_\star}{\sigma_\star} t_{\text{cluster}} \\ &= 0.2 \left(\frac{t_{\text{cluster}}}{20 \text{ Myr}} \right) \left(\frac{a_p}{50 \text{ au}} \right) \left(\frac{M_{\text{tot}}}{2 M_\odot} \right) \\ &\quad \times \left(\frac{n_\star}{10^3 \text{ pc}^{-3}} \right) \left(\frac{\sigma_\star}{1 \text{ km/s}} \right)^{-1}, \end{aligned} \quad (17)$$

where $M_{\text{tot}} = M_1 + M_2$, n_\star is the local stellar density of the cluster, σ_\star its velocity dispersion, and t_{cluster} its lifetime. In equation (16), $f(I_{p,\text{min}})$ measures the overall fraction (for all \tilde{q} values) of close flybys that raise the inclination of the outer planet by $I_p > I_{p,\text{min}}$:

$$f(I_{p,\text{min}}) = \int_0^{+\infty} p(I_p > I_{p,\text{min}}) d\tilde{q}. \quad (18)$$

Note that $f(I_{p,\text{min}})$ can be more than 1, if the requirement $I_p > I_{p,\text{min}}$ is fulfilled for a non-negligible proportion of flybys with q larger than a_p . Figure 5 shows $f(I_{p,\text{min}})$, obtained using the numerical results presented in Figure 4. The function can be approximated by a power-law fit,

$$f(I_{p,\text{min}}) \simeq \frac{7}{(I_{p,\text{min}}/\text{deg})^{0.79}}. \quad (19)$$

We emphasize that the function $f(I_{p,\text{min}})$ is universal, in the sense that it describes the effect of a general parabolic encounter between two equal-mass stars, and can be applied to all m_p and a_p values (assuming $m_p \ll M$). In Section 5, we will apply equations (16) and (19) to “SEs + companion” systems to estimate the likelihood that stellar flybys can destroy the co-transiting geometry of SEs.

4.2 Effect on the eccentricity

Stellar flybys not only change the inclination of the outer planet, but also excite the planet’s eccentricity. Figure 6 shows the joint distribution of I_p and e_p after stellar flybys. The inclination increases are correlated to eccentricity excitations, so that the post-flyby orbit of the planet is not circular. However, its eccentricity will very likely stay low ($e_p \lesssim 0.5$) if

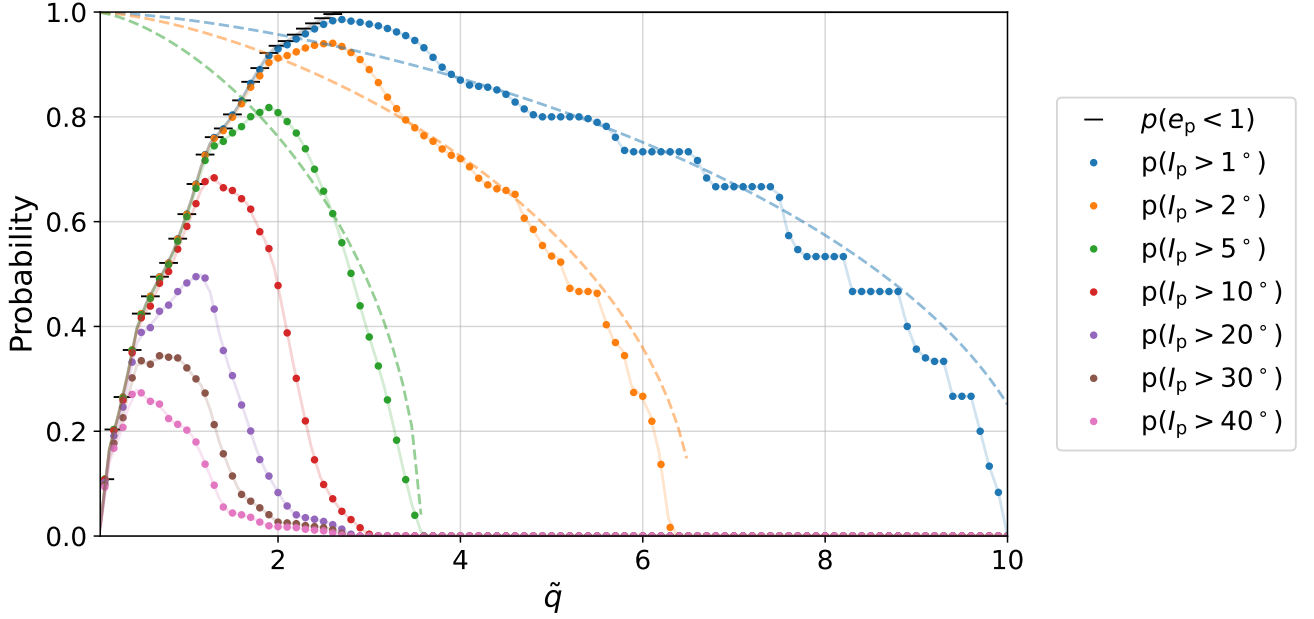


Figure 4. The probability $p(I_p > I_{p,\min})$ for a flyby to raise the inclination of the outer planet to $I_p > I_{p,\min}$ (while keeping the planet bound), as a function of the dimensionless distance at closest approach $\tilde{q} = q/a_p$. Each point is computed from $30 \times 20 \times 20$ N-body simulations that sample the flyby geometry. The dashed lines are the analytical results in the secular approximation (see Appendix for derivation and comparison). The non-smooth features in the blue and orange points are due to the finite numbers of simulations for each \tilde{q} and are not physical. The short bars give $p(e_p > 1)$, the probability that the planet remains bound after the flyby.

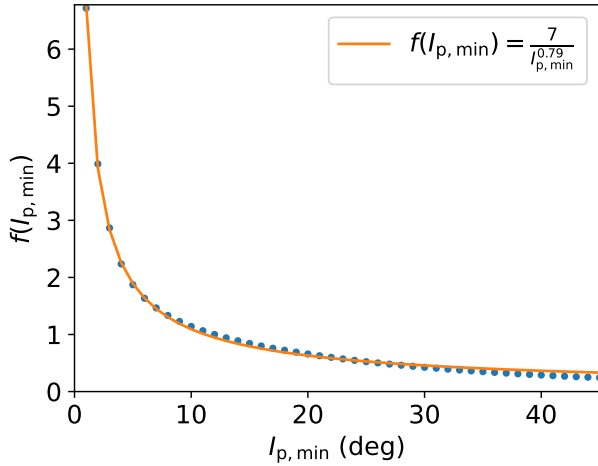


Figure 5. Integrated probability $f(I_{p,\min})$ (equation 18) for stellar flybys to raise the inclination of the outer planet from 0 to $I_p > I_{p,\min}$. The blue dots are computed numerically from Fig. 4, and the orange line is a simple power-law fit given by equation (19).

the inclination gain is small ($I_p \lesssim 5^\circ$). In this case, the inclination dynamics presented in Section 3 is largely unchanged compared to the circular orbit case. When we consider higher I_p , then the eccentricity can become larger. In that case, the stability of the system is not guaranteed, so the inclination dynamics for circular orbit may not hold. In the following

section, we will show that the occurrence rate of our flyby-induced misalignment scenario depends mostly on the statistics for small I_p , so that we can safely ignore the eccentricity's effect on the inclination dynamics.

5 OCCURRENCE RATE OF SUPER-EARTH MISALIGNMENT INDUCED BY STELLAR FLYBYS: SINGLE OUTER PLANET

We now compute the expected number of stellar flybys that generate a misalignment of $\Delta I > \Delta I_{\text{crit}}$ between the SEs as a function of the outer planet's semimajor axis a_p and mass m_p , for given SE and cluster properties. In Section 3, we derived the required $I_{p,\text{crit}}(a_p)$ (see equations 12 & 14) to induce a misalignment ΔI_{crit} given an outer planet at a_p . From equation (16), the number of flybys that produce $\Delta I > \Delta I_{\text{crit}}$ is then

$$\begin{aligned} \mathcal{N}(\Delta I > \Delta I_{\text{crit}}, a_p) &= \mathcal{N}(I_p > I_{p,\text{crit}}(a_p), a_p) \\ &= \mathcal{N}_{\text{close}}(a_p) \times f(I_{p,\min} = I_{p,\text{crit}}(a_p)). \end{aligned} \quad (20)$$

We previously identified two regimes for $I_{p,\text{crit}}(a_p)$ (equations 12 & 14), depending of the coupling parameter $\varepsilon_{12,p}$. These regimes impact how \mathcal{N} scales with the semimajor axis a_p . In the weak coupling regime, $\varepsilon_{12,p} \gtrsim 1$ or $\tilde{a}_p \lesssim (\varepsilon_{12}\tilde{m}_p)^{1/3}$, we have $I_{p,\text{crit}}(a_p) = \Delta I_{\text{crit}}$ and thus

$$\begin{aligned} \mathcal{N}(\Delta I > \Delta I_{\text{crit}}, a_p) &= \mathcal{N}_{\text{close}}(a_p) \times f(I_{p,\min} = \Delta I_{\text{crit}}) \\ &\propto t_{\text{cluster}} n_{\star} \sigma_{\star}^{-1} M_{\text{tot}} a_p (\Delta I_{\text{crit}})^{-0.79}. \end{aligned} \quad (21)$$

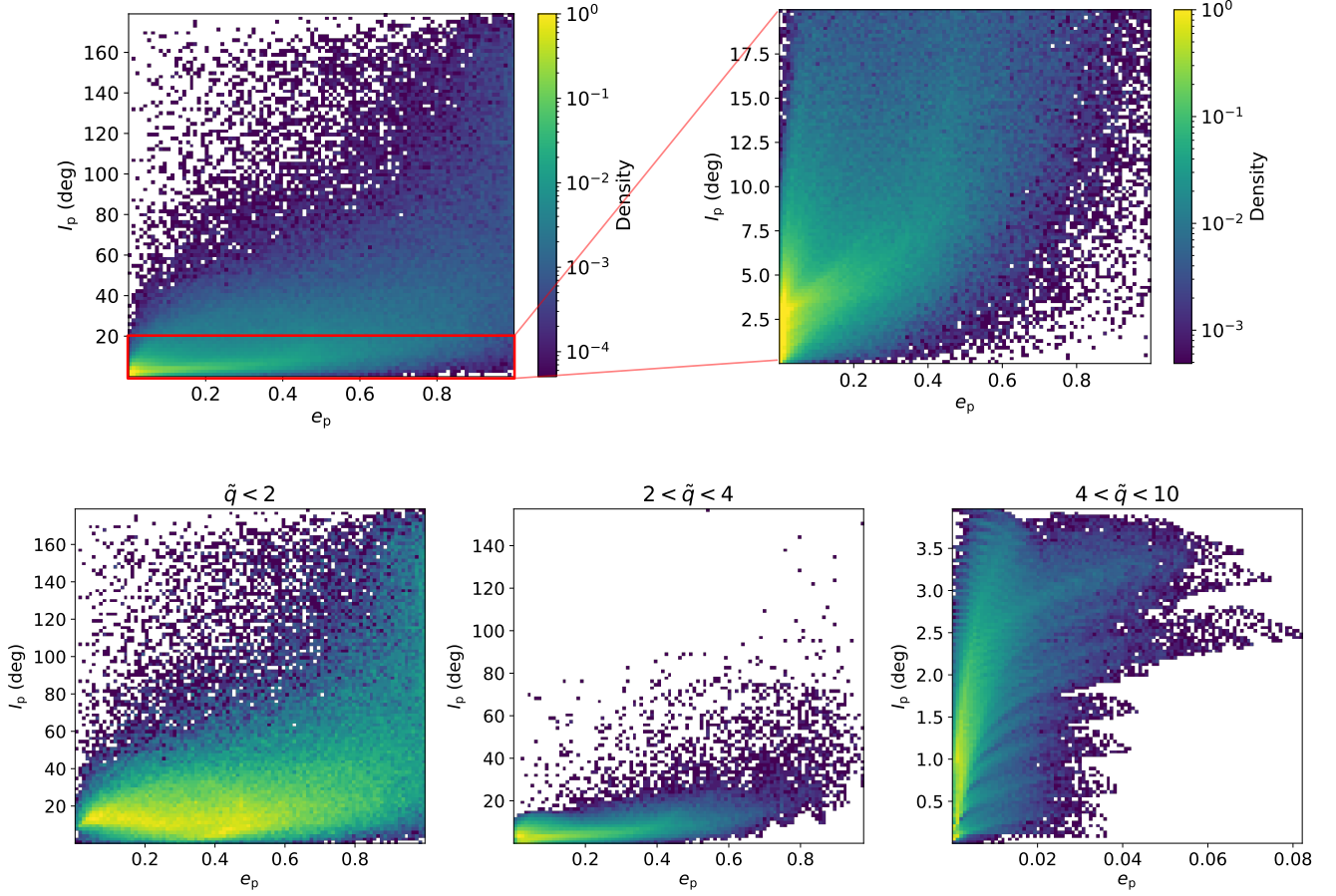


Figure 6. Correlation between the eccentricity e_p and inclination I_p of the outer planet after stellar flybys. The plots are generated from N -body simulations with different flyby geometries and distance at closest approaches, and the color scales logarithmically with the local density of simulations. The plots only show simulations where the planet remains bound. The upper panels gather all flyby distances at closest approach \tilde{q} (with the right panel showing a zoom-in on the low inclination part of the left panel), the lower panels distinguish three different ranges of \tilde{q} . The stripes-like structure in the lower right panel is not physical, and is due to the discrete inclination sampling.

In the strong coupling regime, $\varepsilon_{12,p} \lesssim 1$ or $\tilde{a}_p \gtrsim (\varepsilon_{12}\tilde{m}_p)^{1/3}$, $I_{p,\text{crit}}(a_p)$ is given by equation (14), and assuming $I_{p,\text{crit}}(a_p) \ll 1$ we have

$$\mathcal{N}(\Delta I > \Delta I_{\text{crit}}, a_p) \propto t_{\text{cluster}} n_{\star} \sigma_{\star}^{-1} M_{\text{tot}} a_p^{-1.37} \left(\frac{\varepsilon_{12} m_p}{\Delta I_{\text{crit}}} \right)^{0.79}. \quad (22)$$

Figures 7 and 8 show $\mathcal{N}(\Delta I > 0.5^\circ, a_p)$ as a function of the semimajor axis of the outer planet a_p , for different values of m_p and ε_{12} (which characterizes the coupling of the inner SE system, see equation 7). The two regimes (linear and decreasing power-law dependence of a_p) are clearly visible on the plots. Moreover, there is a maximum $a_{p,\text{max}}$ above which no I_p can induce the required ΔI_{crit} (see equation 15), and thus $\mathcal{N}(\Delta I > \Delta I_{\text{crit}}, a_p) = 0$ for $a_p > a_{p,\text{max}}$.

The maximum of each curve in Figs. 7–8, \mathcal{N}_{max} , is reached at $\varepsilon_{12,p} \simeq 1$, or $\tilde{a}_p \simeq (\varepsilon_{12}\tilde{m}_p)^{1/3}$. It requires a companion inclination I_p no more than ΔI_{crit} , justifying our assumption to neglect the eccentricity effect (see Section 4, Fig. 6). They

are given by

$$a_{p,\text{peak}} \simeq 2.2 \text{ au} \left(\frac{\varepsilon_{12}}{10} \right)^{\frac{1}{3}} \left(\frac{m_p}{1 \text{ M}_J} \right)^{\frac{1}{3}}, \quad (23)$$

$$\mathcal{N}_{\text{max}} \simeq 0.1 \left(\frac{\Delta I_{\text{crit}}}{0.5^\circ} \right)^{-0.79} \left(\frac{\varepsilon_{12}}{10} \right)^{\frac{1}{3}} \left(\frac{m_p}{1 \text{ M}_J} \right)^{\frac{1}{3}} \left(\frac{t_{\text{cluster}}}{20 \text{ Myr}} \right) \times \left(\frac{M_{\text{tot}}}{2 \text{ M}_\odot} \right) \left(\frac{n_{\star}}{10^3 \text{ pc}^{-3}} \right) \left(\frac{\sigma_{\star}}{1 \text{ km.s}^{-1}} \right)^{-1} \quad (24)$$

We recall that ε_{12} varies with a_2^3/m_2 for fixed a_2/a_1 and m_2/m_1 (see equation 7), so that both \mathcal{N}_{max} and $a_{p,\text{peak}}$ are proportional to a_2 , i.e. to the scale of the inner SE system. Figure 9 displays \mathcal{N}_{max} and $a_{p,\text{peak}}$ as a function of ε_{12} for different m_p . Note that since both \mathcal{N}_{max} and $a_{p,\text{peak}}$ scale with $(\varepsilon_{12} m_p)^{1/3}$ in the same way, they can be plotted with the same curves with different vertical scales. From equation (7) and Fig. 2, we see that for typical SE systems, $\varepsilon_{12} = 2.5(a_2/0.2 \text{ au})^3(m_2/10 \text{ M}_\oplus)^{-1}\hat{\varepsilon}_{12}$ and $\hat{\varepsilon}_{12} \sim 1$ (for $a_2/a_1 \sim 2$). Equation (24) and Fig. 9 then indicate $\mathcal{N} \lesssim 0.1$ (subject to uncertainties related to various SE and cluster parameters), suggesting that the co-transiting geometry of

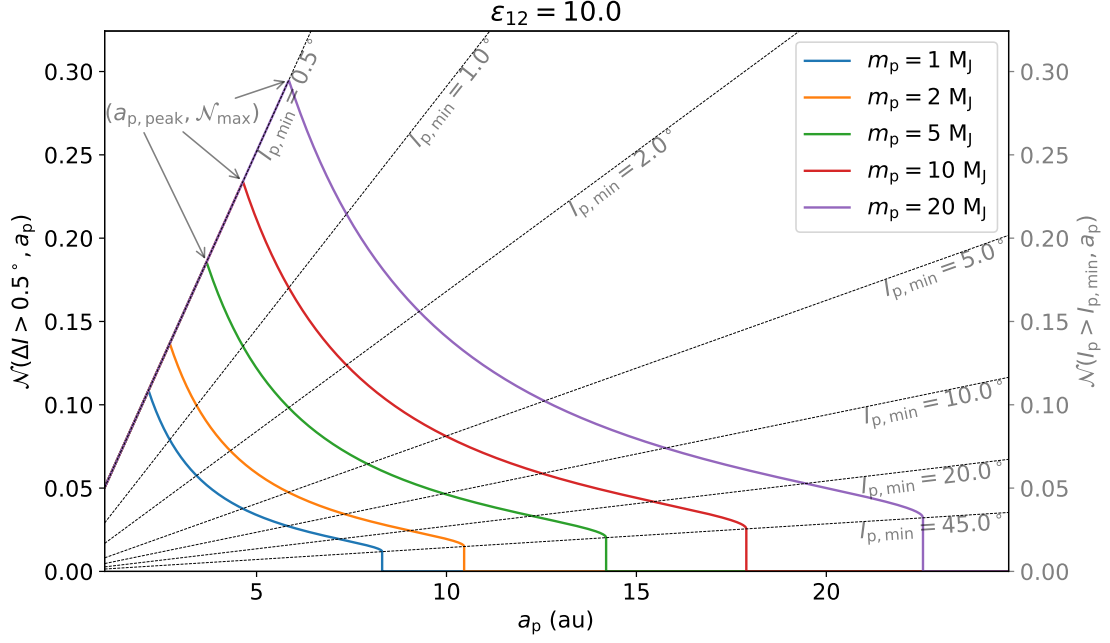


Figure 7. Number of stellar flybys that generate $\Delta I > \Delta I_{\text{crit}} = 0.5^\circ$ in the SE system as a function of a_p of the outer planet companion, for different values of m_p (solid lines; see equations 20,21,22). Each curve terminates at $a_{p,\text{max}}$, given by equation (15). The peak of each curve is located at $(a_{p,\text{peak}}, \mathcal{N}_{\text{max}})$. The inner SE system is characterized by $\epsilon_{12} = 10$ (equation 7), and the cluster parameters are fixed to the fiducial values of equation (17): $t_{\text{cluster}} = 20$ Myr, $\sigma_\star = 1 \text{ km.s}^{-1}$, $n_\star = 10^3 \text{ pc}^{-3}$, and $M_{\text{tot}} = 2M_\odot$. The light dashed lines give $\mathcal{N}(I_p > I_{p,\text{min}}, a_p)$ for different values of $I_{p,\text{min}}$ (see equation 16).

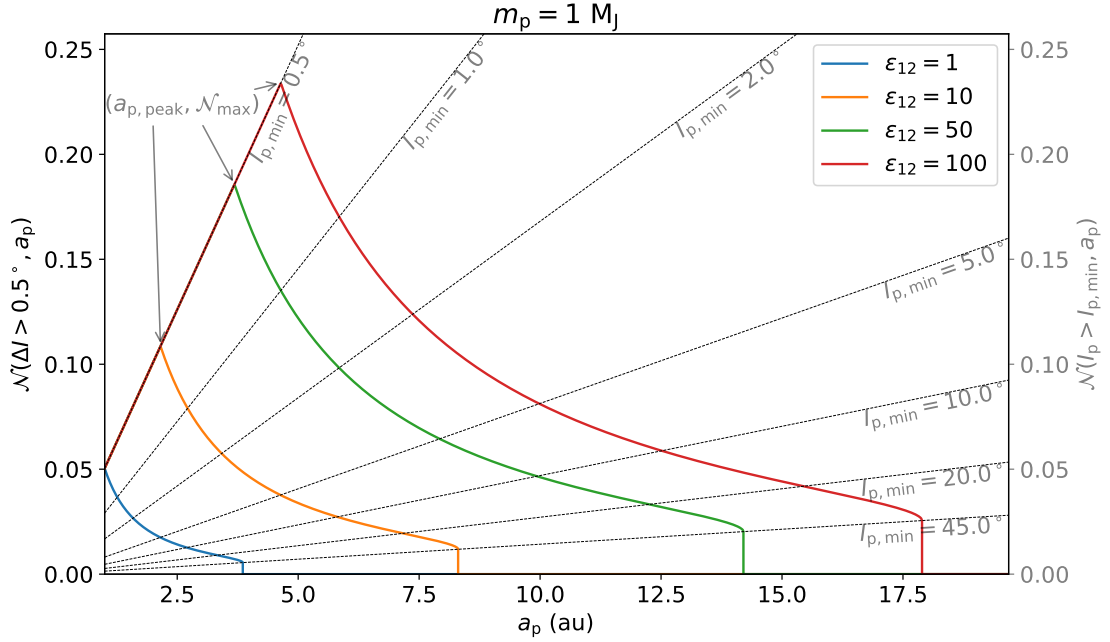


Figure 8. Same as Figure 7, except for a fixed $m_p = 1 M_J$ and different coupling parameter ϵ_{12} (see equation 7) for the inner SE system.

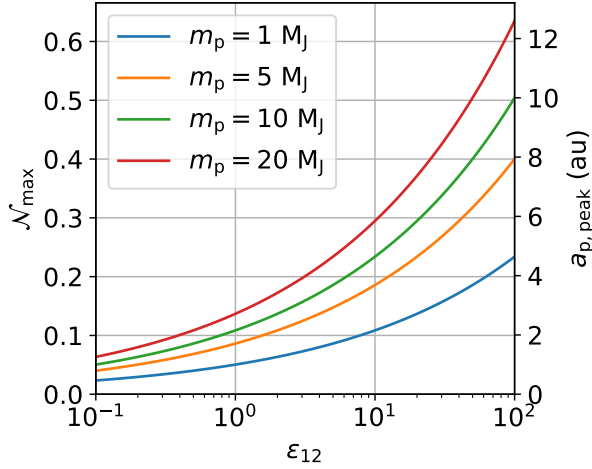


Figure 9. The maximum possible number of flybys \mathcal{N}_{\max} that can produce $\Delta I > 0.5^\circ$ in the SE system and corresponding $a_{p,\text{peak}}$ as a function of ε_{12} , for different m_p (see equations 23–24). The \mathcal{N}_{\max} value uses the cluster parameters $t_{\text{cluster}} = 20$ Myr, $\sigma_\star = 1$ km/s and $n_\star = 10^3$ pc $^{-3}$. \mathcal{N}_{\max} scales with $m_p^{1/3}$, but can be easily rescaled for different parameters (see equation 17) and different m_p (since $\mathcal{N}_{\max} \propto m_p^{1/3}$).

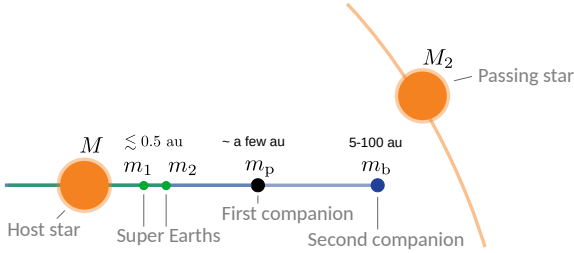


Figure 10. Schematic of the flyby-induced misalignment cascade scenario considered in Section 6: an initially coplanar system comprising two inner planets (SEs) and two outer companions encounters a passing star.

most SE systems is not affected by stellar flybys. In the next section, we will consider how this result changes when SE systems have two external companions.

6 SUPER-EARTH SYSTEMS WITH TWO EXTERIOR COMPANIONS

In the previous section, we have seen that flyby-induced misalignment of SEs by way of a single outer companion/planet is somewhat inefficient (see equation 24). In this section we add a second companion m_b in a circular orbit (semimajor axis a_b) around the host star (see Fig. 10). This second companion can be farther away, thus increasing the effect cross section for flybys. The flyby-induced misalignment I_b on this second companion will misalign the first companion by I_p , which will then increase the mutual inclination ΔI between the SEs.

Equations (9)–(10) giving the forced mutual inclination ΔI of the SEs as a function of the misalignment I_p of the first companion are still valid. However, I_p is not a direct product of the flyby anymore: it is induced by the misalignment of the second companion m_b . The relationship between I_p and I_b is controlled by a new coupling parameter $\varepsilon_{12p,b}$, which characterizes the forcing strength of the second companion on the inner (SEs+ m_p) system compared to the mutual coupling between the SEs and m_p . To evaluate this parameter, we note that when the two SEs are strongly coupled, we can treat them as a single body (denoted by $\bar{12}$), and their orbital axis $\mathbf{L}_{\bar{12}} = \mathbf{L}_1 + \mathbf{L}_2$ precesses around \mathbf{L}_p with the characteristic frequency

$$\omega_{\bar{12}p} = \frac{L_1\omega_{1p} + L_2\omega_{2p}}{L_1 + L_2}, \quad (25)$$

where ω_{1p} and ω_{2p} are given by equations (3)–(4). For $a_1, a_2 \ll a_p$, we can define the effective semi-major axis of $\bar{12}$ via [see Eqs 3–4 with $b_{3/2}^{(1)}(\alpha) \simeq 3\alpha$]

$$\omega_{\bar{12}p} \simeq \frac{3}{4}n_{12} \frac{m_p}{M} \left(\frac{a_{\bar{12}}}{a_p}\right)^3 = \frac{3}{4}\sqrt{\frac{GM}{a_{12}^3}} \frac{m_p}{M} \left(\frac{a_{\bar{12}}}{a_p}\right)^3, \quad (26)$$

which gives

$$a_{\bar{12}} = \left(\frac{m_1 a_1^2 + m_2 a_2^2}{m_1 \sqrt{a_1} + m_2 \sqrt{a_2}}\right)^{\frac{2}{3}}. \quad (27)$$

Similarly, the characteristic precession rate of $\mathbf{L}_{\bar{12}}$ around \mathbf{L}_b is given by

$$\omega_{\bar{12}b} = \frac{L_1\omega_{1b} + L_2\omega_{2b}}{L_1 + L_2} = \frac{3}{4}n_{12} \frac{m_b}{M} \left(\frac{a_{\bar{12}}}{a_b}\right)^3. \quad (28)$$

Thus, analogous to equation (6), we can define the coupling parameter

$$\varepsilon_{\bar{12}p,b} = \frac{\omega_{pb} - \omega_{\bar{12}b}}{\omega_{\bar{12}p} + \omega_{p\bar{12}}} \simeq \frac{\omega_{pb}}{\omega_{\bar{12}p}} = \frac{m_b}{m_p} \left(\frac{a_p}{a_b}\right)^3 \left(\frac{a_p}{a_{\bar{12}}}\right)^{\frac{3}{2}}, \quad (29)$$

where in the second equality we have used $\omega_{p\bar{12}} = (L_{\bar{12}}/L_p)\omega_{\bar{12}p} \ll \omega_{\bar{12}p}$ and $\omega_{\bar{12}b} \ll \omega_{pb}$ —these are valid for $a_{\bar{12}} < a_p \ll a_b$ and $m_1, m_2 \ll m_p, m_b$. When $\varepsilon_{\bar{12}p,b} \ll 1$, then the second companion's influence is weaker than the coupling between the first companion (m_p) and the SEs, and the forced inclination between m_p and the SE system is

$$I_p \simeq \frac{1}{2} \sin(2I_b) \varepsilon_{\bar{12}p,b}. \quad (30)$$

On the other hand, when $\varepsilon_{\bar{12}p,b} \gg 1$, the coupling between m_p and the SEs is negligible and the forced inclination becomes

$$I_p \simeq I_b \quad (31)$$

The finite I_p will then lead to misalignment ΔI between the two SEs (see Section 3). The critical $I_{b,\text{crit}}$ to induce a misalignment ΔI_{crit} between the SEs depends on the two coupling parameters, $\varepsilon_{12,p}$ and $\varepsilon_{\bar{12}p,b}$. This leads to four regimes (Fig. 11):

- (i) $\varepsilon_{12,p} \gtrsim 1$ and $\varepsilon_{\bar{12}p,b} \gtrsim 1$

The first companion m_p has a strong influence on the SEs, and the second companion m_b has a strong influence on the inner "SEs+ m_p " system. The misalignment I_b of m_b generated by a flyby is then directly transmitted to m_p and the SEs (i.e. $\Delta I \simeq I_p \simeq I_b$).



Figure 11. Schematic of the four different regimes characterized by the coupling parameters $\varepsilon_{12,p}$ (see equation 6) and $\varepsilon_{12p,b}$ (see equation 29). When $\varepsilon_{12,p} \gtrsim 1$ ($\lesssim 1$), the first companion m_p has a stronger (weaker) influence on the SEs (m_1 and m_2) compared to the mutual coupling between m_1 and m_2 ; when $\varepsilon_{12p,b} \gtrsim 1$ ($\lesssim 1$), the second companion m_b has a stronger (weaker) influence on the inner "SEs+ m_p " system compared to the mutual coupling between the SEs and m_p . In this schematic, a companion is strong if its distance to the inner bodies is similar to the distance between the inner bodies or if it is much more massive.

(ii) $\varepsilon_{12,p} \lesssim 1$ and $\varepsilon_{12p,b} \gtrsim 1$

The first companion has a weak influence on the SEs, but the second companion has a strong influence on the inner system. The misalignment of m_b is directly transmitted to m_p (ie $I_p \simeq I_b$), but the mutual inclination ΔI of the SEs is reduced from I_p (see equation 9).

(iii) $\varepsilon_{12,p} \gtrsim 1$ and $\varepsilon_{12p,b} \lesssim 1$

The first companion has a strong influence on the SEs, but the second companion has a weak influence on the inner system. The misalignment I_p of m_p is then reduced from I_b , while it is directly transmitted to the SEs (ie $\Delta I \simeq I_p$).

(iv) $\varepsilon_{12,p} \lesssim 1$ and $\varepsilon_{12p,b} \lesssim 1$

The first companion has a weak influence on the SEs, and the second companion also has a weak influence on the inner system. The misalignment of m_p is then reduced from I_b , and the mutual inclination of the SEs is also reduced from I_p .

The expression of $I_{b,crit}$ in each regime is

$$I_{b,crit} \simeq \begin{cases} \Delta I_{crit} & \text{Regime 1} \\ \frac{1}{2} \arcsin\left(\frac{2\Delta I_{crit}}{\varepsilon_{12,p}}\right) & \text{Regime 2} \\ \frac{1}{2} \arcsin\left(\frac{2\Delta I_{crit}}{\varepsilon_{12p,b}}\right) & \text{Regime 3} \\ \frac{1}{2} \arcsin\left(\frac{1}{\varepsilon_{12p,b}} \arcsin\left(\frac{2\Delta I_{crit}}{\varepsilon_{12,p}}\right)\right) & \text{Regime 4} \end{cases} \quad (32)$$

The maximum possible value for the semimajor axis of the first companion derived in equation (15) still holds, i.e.

$$\tilde{a}_{p,max} = \left(\frac{\varepsilon_{12}\tilde{m}_p}{2\Delta I_{crit}}\right)^{\frac{1}{3}}. \quad (33)$$

In addition, there is a maximum value of a_b beyond which $\Delta I > \Delta I_{crit}$ can never be produced; this $a_{b,max}$ is set by $I_{p,crit} = \varepsilon_{12p,b}/2$, with $I_{p,crit}$ given by equations (12) and (14), depending on whether $\varepsilon_{12,p} \gtrsim 1$ or $\varepsilon_{12,p} \lesssim 1$. Thus we have

$$a_{b,max} = \begin{cases} a_p \left(\frac{a_p}{a_{12}}\right)^{\frac{1}{2}} \left(\frac{m_b}{m_p} \frac{1}{2\Delta I_{crit}}\right)^{\frac{1}{3}} & \text{if } \varepsilon_{12,p} \gtrsim 1 \\ a_p \left(\frac{a_p}{a_{12}}\right)^{\frac{1}{2}} \left(\frac{m_b}{m_p} \frac{\varepsilon_{12,p}}{2\Delta I_{crit}}\right)^{\frac{1}{3}} & \text{if } \varepsilon_{12,p} \lesssim 1 \end{cases} \quad (34)$$

Using equation (16) (but applied to the outermost companion m_b), we find that the number of flybys that can produce

$\Delta I > \Delta I_{crit}$ is

$$\begin{aligned} \mathcal{N}(\Delta I > \Delta I_{crit}, a_b) &= \mathcal{N}(I_b > I_{b,crit}(a_b), a_b) \\ &= \mathcal{N}_{close}(a_b) \times f(I_{b,min} = I_{b,crit}(a_b)). \end{aligned} \quad (35)$$

Figures 12–13 show $\mathcal{N}(\Delta I > \Delta I_{crit}, a_b)$ as a function of a_b , for given m_b, m_p, a_p , and SE properties ε_{12} and a_{12} , for the cases of $\varepsilon_{12,p} \gtrsim 1$ and $\varepsilon_{12,p} \lesssim 1$, respectively. For a given a_p , the maximum number of flybys $\mathcal{N}_{max}(a_p)$ occurs when $\varepsilon_{12p,b} \sim 1$. The corresponding $a_{b,peak}$ and $\mathcal{N}_{max}(a_p)$ are

$$a_{b,peak} = a_p \left(\frac{a_p}{a_{12}}\right)^{\frac{1}{2}} \left(\frac{m_b}{m_p}\right)^{\frac{1}{3}} \quad (36)$$

$$\mathcal{N}_{max} = \mathcal{N}_{close}(a_{b,peak}) \times f(I_{p,crit}) \propto a_{b,peak}. \quad (37)$$

Figure 14 displays $\mathcal{N}_{max}(a_p)$ and the corresponding $a_{b,peak}$ as a function of a_p , for two different ε_{12} (recall that ε_{12} characterizes the architecture of the inner SE system; see Fig. 2). Note that $\mathcal{N}_{max}(a_p)$ has a peak value, reached when $a_p = a_{p,peak}$, corresponding to the transition between regimes where $\varepsilon_{12,p} \lesssim 1$ and $\varepsilon_{12,p} \gtrsim 1$. In other words, for each SE system, there is an optimal companion architecture ($a_{p,peak}, a_{b,peak}$) that maximizes the number of effective flybys $\mathcal{N}_{max} = \mathcal{N}_{max,peak}$, which occurs when both $\varepsilon_{12,p}$ and $\varepsilon_{12p,b}$ are approximately equal to 1. Requiring both coupling ratios to be 1, $a_{p,peak}$ is given by equation (23),

$$a_{p,peak} = (\varepsilon_{12}\tilde{m}_p)^{1/3} \text{ au}, \quad (38)$$

and $a_{b,peak}$ is given by equation (36) with $a_p = a_{p,peak}$:

$$a_{b,peak} = \left(\frac{\varepsilon_{12}}{\tilde{a}_{12}}\right)^{\frac{1}{2}} (\tilde{m}_p \tilde{m}_b^2)^{\frac{1}{6}} \text{ au}, \quad (39)$$

where $\tilde{a}_{12} \equiv a_{12}/(1 \text{ au})$ and $\tilde{m}_b \equiv m_b/(1 M_J)$. For a typical system with Earth-mass planets, a cold Jupiter and an outer brown dwarf, we have

$$a_{b,peak} \simeq 16 \text{ au} \left(\frac{\varepsilon_{12}}{10}\right)^{\frac{1}{2}} \left(\frac{m_p}{1 M_J}\right)^{\frac{1}{6}} \left(\frac{m_b}{50 M_J}\right)^{\frac{1}{3}} \left(\frac{a_{12}}{0.5 \text{ au}}\right)^{-\frac{1}{2}}. \quad (40)$$

The corresponding $\mathcal{N}_{max,peak}$ is

$$\begin{aligned} \mathcal{N}_{max,peak} &= \mathcal{N}_{close}(a_{b,peak}) \times f(\Delta I_{crit}) \\ &\simeq 0.8 \left(\frac{\Delta I_{crit}}{0.5^\circ}\right)^{-0.79} \left(\frac{\varepsilon_{12}}{10}\right)^{\frac{1}{2}} \left(\frac{m_p}{1 M_J}\right)^{\frac{1}{6}} \\ &\quad \times \left(\frac{m_b}{50 M_J}\right)^{\frac{1}{3}} \left(\frac{a_{12}}{0.5 \text{ au}}\right)^{-\frac{1}{2}} \left(\frac{t_{cluster}}{20 \text{ Myr}}\right) \\ &\quad \times \left(\frac{M_{tot}}{2 M_\odot}\right) \left(\frac{n_\star}{10^3 \text{ pc}^{-3}}\right) \left(\frac{\sigma_\star}{1 \text{ km/s}}\right)^{-1}. \end{aligned} \quad (41)$$

This maximal "peak" number of flybys is shown in Figure 15, along with the optimal semimajor axes of the two companions. The result depends on the SE systems through now two parameters, ε_{12} and a_{12} . Using equation (8), we can rewrite equation (37) to understand the dependence on $\mathcal{N}_{max,peak}$ on

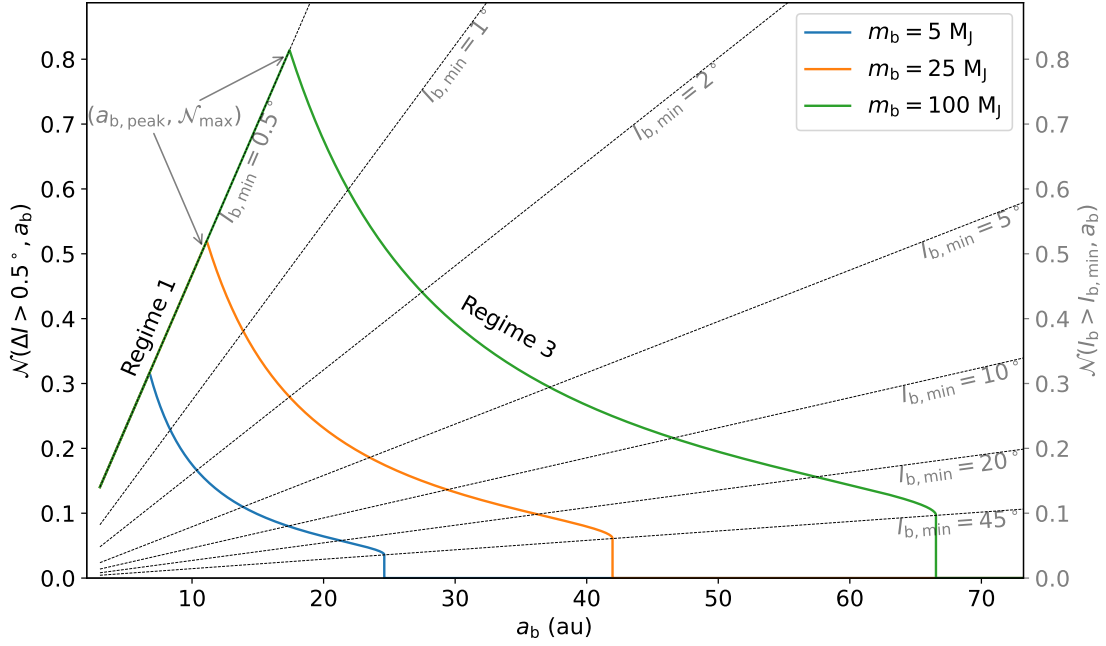


Figure 12. Number of stellar flybys that generate $\Delta I \gtrsim \Delta I_{\text{crit}} = 0.5^\circ$ in the SE system as a function of a_b of the outermost companion, for different values of m_b (solid lines; see equation 35). Each curve terminates at $a_{b,\text{max}}$, given by equation (34). The inner SE system is characterized by $\varepsilon_{12} = 10$ (equation 7), $a_{12} = 0.5$ au, and the inner companion's parameters are fixed to $a_p = 2$ au and $m_p = 1 M_J$, so that $\varepsilon_{12,p} \gtrsim 1$. This situation corresponds to regimes 1 (for small a_b) and 3 (for high a_b). The cluster parameters are fixed to the fiducial values of equation (17): $t_{\text{cluster}} = 20$ Myr, $\sigma_\star = 1$ km/s and $n_\star = 10^3 \text{ pc}^{-3}$. The light dashed lines give $\mathcal{N}(I_b > I_{b,\text{min}}, a_b)$ for different values of $I_{b,\text{min}}$ (see equation 16, applied to the outermost companion). See Figures 7–8 for the cases of SEs with a single companion.

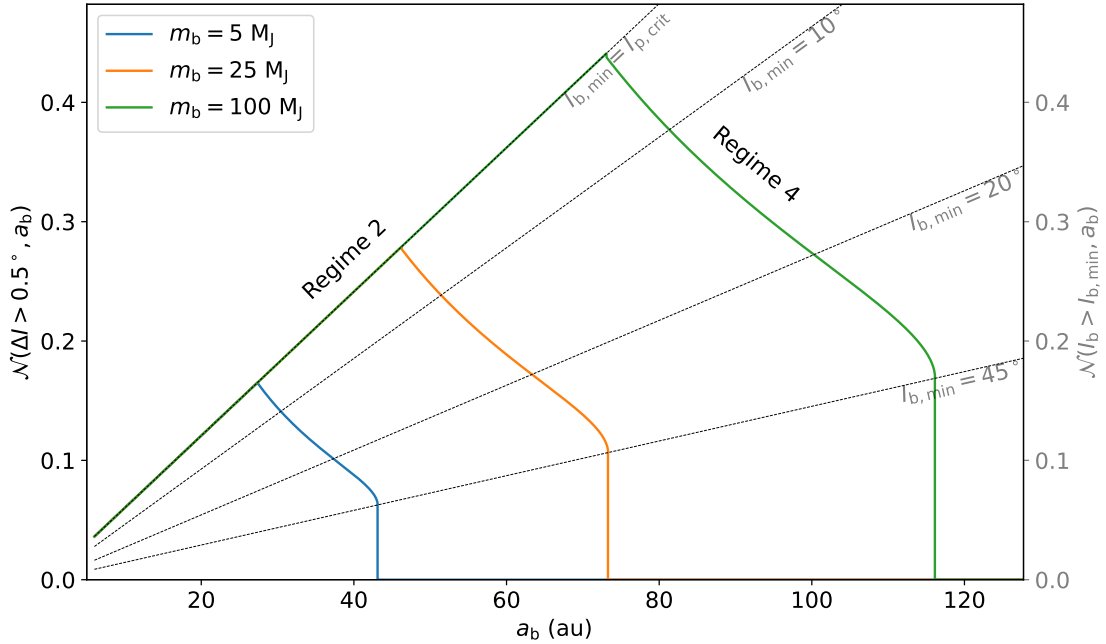


Figure 13. Same as Figure 12, except for $a_p = 5$ au, corresponding to $\varepsilon_{12,p} = 0.07$ (see equation 7). For this value of the coupling parameter, the first companion m_p should have a minimum $I_{p,\text{crit}} \sim 7^\circ > \Delta I_{\text{crit}}$ (see equation 14) to generate a misalignment $\Delta I > \Delta I_{\text{crit}}$ within the inner SE system. This case corresponds to regimes 2 (for small a_b) and 4 (for high a_b).

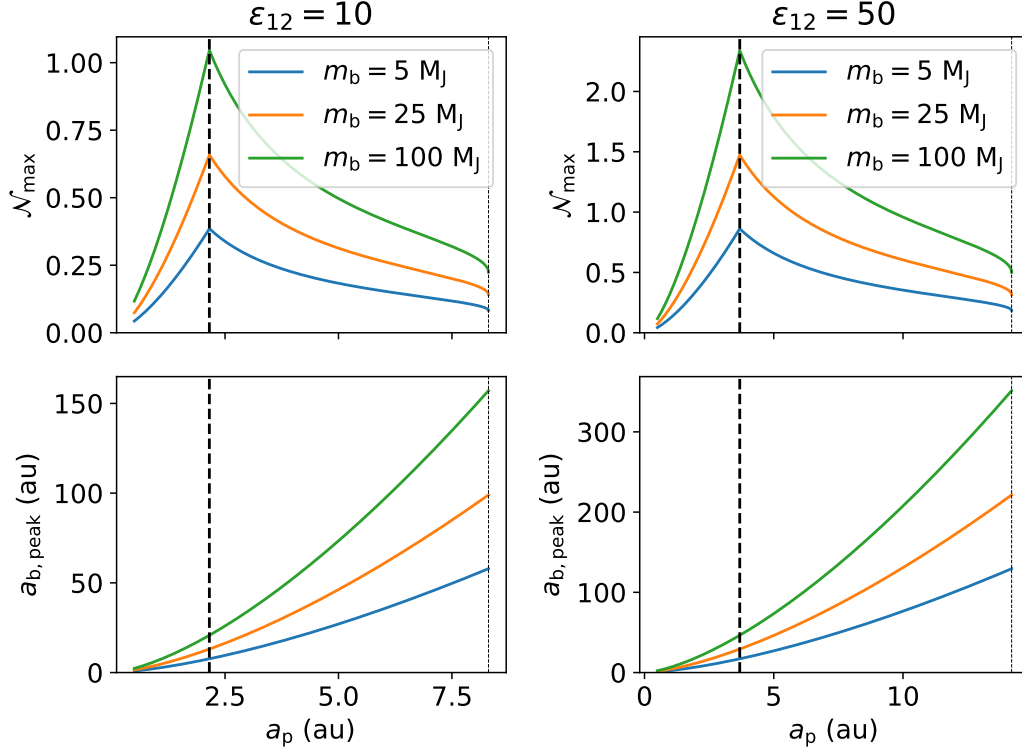


Figure 14. Maximum number of flybys \mathcal{N}_{\max} that gives $\Delta I \gtrsim \Delta I_{\text{crit}} = 0.5^\circ$ (top) and optimal $a_{b,\text{peak}}$ (bottom) as a function of a_p (equation 37), for different values of m_b . Note that $a_{b,\text{peak}}$ is chosen so as to maximize the number of flybys, i.e. such that $\varepsilon_{12p,b} = 1$ (equation 36). The optimal a_p is indicated with a dashed vertical line: it corresponds to $\varepsilon_{12,p} = 1$ and does not depend on m_b . The maximum a_p at around 8 au (left) or 15 au (right) is similarly independent of m_b (equation 15). The SEs system is fixed, with $\varepsilon_{12} = 10$ (left) and $\varepsilon_{12} = 50$ (right), $a_{12} = 0.5$ au, and the mass of the first companion is fixed to $m_p = 1 M_J$. The cluster parameters are $t_{\text{cluster}} = 20$ Myr, $\sigma_\star = 1$ km/s and $n_\star = 10^3 \text{ pc}^{-3}$. Note that \mathcal{N}_{\max} scales with $a_{12}^{-1/2}$ and $m_p^{-1/3}$, and is proportional to t_{cluster} , σ_\star^{-1} , and n_\star .

various parameters:

$$\begin{aligned} \mathcal{N}_{\max,\text{peak}} \simeq & 0.8 \left(\frac{\Delta I_{\text{crit}}}{0.5^\circ} \right)^{-0.79} \left(\frac{\hat{\varepsilon}_{12}}{10} \right)^{\frac{1}{2}} \left(\frac{m_2}{10 M_J} \right)^{-\frac{1}{2}} \\ & \times \left(\frac{a_2}{10 \text{ au}} \right)^{\frac{3}{2}} \left(\frac{a_{12}}{0.5 \text{ au}} \right)^{-\frac{1}{2}} \left(\frac{m_p}{1 M_J} \right)^{\frac{1}{6}} \left(\frac{m_b}{50 M_J} \right)^{\frac{1}{3}} \\ & \times \left(\frac{t_{\text{cluster}}}{20 \text{ Myr}} \right) \left(\frac{M_{\text{tot}}}{2 M_\odot} \right) \left(\frac{n_\star}{10^3 \text{ pc}^{-3}} \right) \left(\frac{\sigma_\star}{1 \text{ km/s}} \right)^{-1}. \end{aligned} \quad (42)$$

Thus, the maximal "peak" number of effective flybys scales linearly with the SEs semi-major axes. Comparing Figures 9 and 15, we see that adding a second companion strongly increases the number of flybys able to break the co-transiting geometry of the inner SEs. Of course, this increase may be tampered by the lower probability of having a suitable two-companion system instead of an one-companion system.

7 SUMMARY AND CONCLUSION

In this paper, we have studied a new mechanism for dynamical excitations of Super-Earths (SE) systems following a close stellar encounter. We are motivated by the recently

claimed correlation between the multiplicity observed in Kepler transiting systems and stellar overdensities (Longmore et al. 2021). The proposed mechanism consists of stellar flybys exciting the inclinations of one or two exterior companion giant planets (or brown dwarfs), which would then induce misalignment in an initially coplanar SE system. Even a modest misalignment ($\Delta I \gtrsim 0.5^\circ$) could break the co-transiting geometry of the SEs, resulting in an apparent excess of single-transiting systems. We study two cases: in one, the SE system has a cold Jupiter companion at a few au; in the other, the SE system has two companions, a cold Jupiter and a wider planetary or substellar companion. Our results can be rescaled easily with the SE system or companion properties.

To evaluate the probability for a system to experience such an "effective" flyby (that can generate $\Delta I \gtrsim 0.5^\circ$ for the SEs), we combine analytical calculation (on stellar encounters and the secular coupling between the SEs and companions) with N -body simulations (to evaluate the effects of representative close encounters). Given the large parameter space and related uncertainties, we have attempted to present our results in an analytical or semi-analytical way, so that they can be rescaled easily for different SE and companion properties and stellar cluster parameters.

When the SE system only has one planetary companion, we show that the mechanism is relatively ineffective. If the

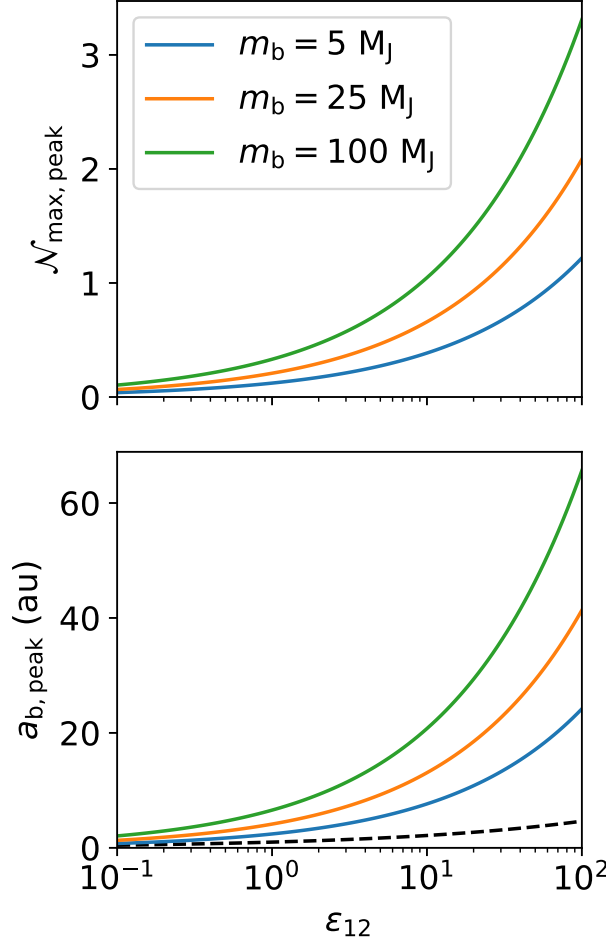


Figure 15. Maximal "peak" number of flybys $\mathcal{N}_{\text{max,peak}}$ that gives $\Delta I \gtrsim \Delta I_{\text{crit}} = 0.5^\circ$ (top) and corresponding $a_{\text{b,peak}}$ (bottom) as a function of ε_{12} (equations 41–42), for different values of m_b . The optimal a_p and a_b values, $a_{\text{p,peak}}$ and $a_{\text{b,peak}}$, are set by $\varepsilon_{12\text{p}} = 1$ and $\varepsilon_{12\text{p,b}} = 1$ (equations 38–39), so as to maximize the number of flybys. The optimal $a_{\text{p,peak}}$ is indicated with a dashed black line on the bottom plot—it does not depend on m_b . The SEs location is set to $a_{12} = 0.5$ au, and the mass of the first companion is fixed to $m_p = 1 M_J$. The cluster properties are $t_{\text{cluster}} = 20$ Myr, $\sigma_\star = 1$ km/s and $n_\star = 10^3 \text{ pc}^{-3}$, but note that $\mathcal{N}_{\text{max,peak}}$ scales with $a_{12}^{-1/2}$ and $m_p^{1/6}$, and is proportional to t_{cluster} , σ_\star^{-1} , and n_\star .

outer planet is close to the SEs, then stellar flybys will have a small chance of changing its orbital inclination. On the other hand, if the outer planet is farther away, then it will have little impact on the SE dynamics, and on their transiting geometry in particular. This trade-off is shown in Figures 7 and 8. For given density, velocity dispersion, and lifetime of the stellar cluster, we can evaluate the expected number of stellar flybys that will disrupt the co-transiting geometry of the SEs as a function of the SE system (characterized by the coupling parameter ε_{12} , equation 7) and the companion properties (semi-major axis and mass). Fixing all parameters but the companion semi-major axis (a_p), the number of “effective” flybys peaks for an optimal a_p which, for typical Kepler SEs, corresponds to a few astronomical units for $m_p \sim 1 M_J$ (see equation 23). The corresponding maximum number of effective flybys and its dependencies in all related parameters is displayed in equation (24). With only one companion, this flyby-induced misalignment scenario is unlikely

to produce statistically significant effect of the SE multiplicity; even when assuming a high cluster density, less than 1 in 10 systems will experience the required stellar flyby.

When the SE system has two companions, the effective cross section for stellar flybys increases. The misalignment induced on the outermost (second) companion m_b by the flyby can be transmitted to the inner (first) companion m_p , which would then be able to break the co-transiting geometry of the SEs. A relatively close (small a_b) second companion would have a strong influence on the inner system (SEs and m_p) (characterized by the parameter $\varepsilon_{12\text{p,b}}$, equation 29), and transmit its misalignment I_b fully to the first companion (i.e. $I_b \sim I_p$ for $\varepsilon_{12\text{p,b}} \gtrsim 1$). On the other hand, a far-out second companion has a better chance of experiencing close stellar flybys, but could have a smaller effect on the inner system. The trade-off is shown in Figures 12 and 13 for two different locations of the first companion, close to the SEs or farther away. Fixing the properties of the SEs, the num-

ber of effective flybys peaks for an optimal combination of a_p and a_b which, for typical Kepler “SE+cold Jupiter systems”, corresponds to a few AU and tens of AU, respectively, for substellar second companions. The corresponding number of flybys and its dependencies on various parameters is displayed in equation (41). The optimal architecture (semi-major axes of the two companions as a function of their masses and the SE parameters) is described in equations (38)–(39) (see Figures 14–15).

Our calculations show that the number of effective flybys (that can generate $\Delta I > 0.5^\circ$ for the SEs) increases significantly when a second companion is added, suggesting that most initially coplanar SE systems with two companions in stellar overdensities will experience a flyby that will misalign their orbits, and thus break the co-transiting geometry. However, SE systems with two companions may be rarer than their one-companion counterparts. Ultimately, further information on the correlation between inner SE systems and substellar companions will be needed to determine the relative prevalence of the mechanisms studied in this paper. Moreover, a deeper knowledge on the properties of stellar birth clusters (lifetime and density in particular) and their relation to the observed overdensities characterized in Winter et al. (2020) and Longmore et al. (2021) is needed to conclude on the role of the flyby-induced misalignment scenario on planetary system architectures.

ACKNOWLEDGEMENTS

This work has been supported in part by the NSF grant AST-17152 and NASA grant 80NSSC19K0444. We made use of the PYTHON libraries NUMPY (Harris et al. 2020), SCIPY (Virtanen et al. 2020), and PYQT-FIT, and the figures were made with MATPLOTLIB (Hunter 2007).

DATA AVAILABILITY

The output of the N -body flyby simulations (Section 4) can be found on <https://github.com/LaRodet/FlybySimulations.git>. All the figures can be directly reproduced from this dataset and from the equations.

REFERENCES

Becker J. C., Adams F. C., 2017, *MNRAS*, 468, 549
 Boué G., Fabrycky D. C., 2014, *ApJ*, 789, 111
 Bryan M. L., et al., 2020, *AJ*, 159, 181
 Cai M. X., Kouwenhoven M. B. N., Zwart S. F. P., Spurzem R., 2017, *MNRAS*
 Carrera D., Davies M. B., Johansen A., 2016, *MNRAS*, 463, 3226
 Denham P., Naoz S., Hoang B.-M., Stephan A. P., Farr W. M., 2019, *MNRAS*, 482, 4146
 Fabrycky D. C., et al., 2014, *ApJ*, 790, 146
 Gaia Collaboration et al., 2018, *A&A*, 616, A1
 Hansen B. M. S., 2017, *MNRAS*, 467, 1531
 Harris C. R., et al., 2020, *Nature*, 585, 357
 He M. Y., Ford E. B., Ragozzine D., 2019, *MNRAS*, 490, 4575
 Huang C. X., Petrovich C., Deibert E., 2017, *AJ*, 153, 210
 Hunter J. D., 2007, *Comput Sci Eng*, 9, 90
 Johansen A., Davies M. B., Church R. P., Holmelin V., 2012, *ApJ*, 758, 39

Lai D., Pu B., 2017, *AJ*, 153, 42
 Laughlin G., Adams F. C., 1998, *ApJ*, 508, L171
 Li D., Mustill A. J., Davies M. B., 2020, *MNRAS*, 496, 1149
 Lissauer J. J., et al., 2011, *ApJS*, 197, 8
 Liu B., Lai D., 2018, *ApJ*, 863, 68
 Longmore S. N., Cheavance M., Kruijssen J. M. D., 2021, *ApJ*, 911, L16
 Malmberg D., Davies M. B., Heggie D. C., 2011, *MNRAS*, 411, 859
 Millholland S. C., He M. Y., Ford E. B., Ragozzine D., Fabrycky D., Winn J. N., 2021, arXiv e-prints, p. arXiv:2106.15589
 Murray C. D., Dermott S. F., 2000, *Solar System Dynamics*. Cambridge University Press
 Mustill A. J., Davies M. B., Johansen A., 2017, *MNRAS*, 468, 3000
 Parker R. J., Quanz S. P., 2012, *MNRAS*, 419, 2448
 Pu B., Lai D., 2018, *MNRAS*, 478, 197
 Pu B., Lai D., 2020, arXiv e-prints, 2008, arXiv:2008.05698
 Read M. J., Wyatt M. C., Triaud A. H. M. J., 2017, *MNRAS*, 469, 171
 Rodet L., Lai D., 2021, *MNRAS*, 502, 3746
 Rodet L., Su Y., Lai D., 2021, *ApJ*, 913, 104
 Virtanen P., et al., 2020, *NatureMethods*, 17, 261
 Wang Y.-H., Leigh N. W. C., Perna R., Shara M. M., 2020, *ApJ*, 905, 136
 Winn J. N., Fabrycky D. C., 2015, *ARA&A*, 53, 409
 Winter A. J., Kruijssen J. M. D., Longmore S. N., Cheavance M., 2020, *Nature*, 586, 528
 Zhu W., Wu Y., 2018, *AJ*, 156, 92
 Zhu W., Petrovich C., Wu Y., Dong S., Xie J., 2018, *ApJ*, 860, 101

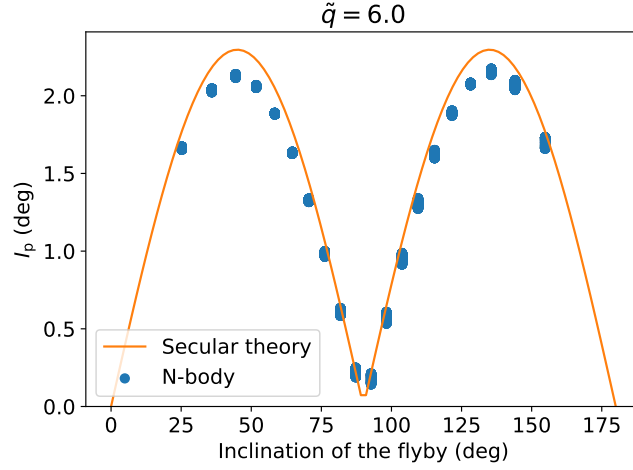


Figure A1. Inclination of the planet after the flyby, from the secular theory (orange, equation A4) and N -body simulations (blue). Each of the 30 simulated inclinations groups 20×20 simulations, with various ω and λ_p .

APPENDIX A: SECULAR PERTURBATION ON THE INCLINATION BY A PARABOLIC FLYBY

The probability $p(I_p > I_{p,\min})$ for a planet m_p to gain an inclination $I_p > I_{p,\min}$ after a parabolic flyby can be computed in the secular framework, for $\tilde{q} \equiv q/a_p \gtrsim 3$. Let us first compute the evolution of the unit angular momentum vector $\hat{\mathbf{L}}_p$ of an initially circular planet orbit (with semi-major axis a_p and mean-motion n_p). Using the secular approach, averaging over the planet's orbit, we get (Eq. 28 in Liu & Lai (2018)):

$$\frac{d\hat{\mathbf{L}}_p}{dt} = -\frac{3n_p M_2 a_p^3}{2M_1 R^3} (\hat{\mathbf{L}}_p \cdot \hat{\mathbf{R}}) (\hat{\mathbf{L}}_p \times \hat{\mathbf{R}}), \quad (\text{A1})$$

where \mathbf{R} represents the instantaneous position of M_2 relative to M_1 , and $\hat{\mathbf{R}} = \mathbf{R}/R$. We choose the xy plane as the plane of the parabolic stellar encounter, with the x axis pointing towards the periastron. We assume that $\hat{\mathbf{L}}_p$ remains close to its initial value throughout the flyby. Integrating $\frac{d\hat{\mathbf{L}}_p}{dt}$ along the parabolic trajectory of the flyby, we find that the change in $\hat{\mathbf{L}}_p$ is given by

$$\delta\hat{\mathbf{L}}_p = \frac{3\pi M_2}{8\sqrt{2M_1(M_1 + M_2)}} \left(\frac{a_p}{q}\right)^{\frac{3}{2}} \sin(2i) \begin{pmatrix} \cos \Omega \\ \sin \Omega \\ 0 \end{pmatrix}, \quad (\text{A2})$$

where i and Ω are respectively the inclination and longitude of the node of the initial orbit of the planet. Thus, the change in the planet's inclination is

$$I_p \simeq |\delta\hat{\mathbf{L}}_p| = \frac{3\pi}{8} \frac{M_2}{\sqrt{2M_1(M_1 + M_2)}} \left(\frac{a_p}{q}\right)^{\frac{3}{2}} \sin(2i) \equiv I_{\max}(\tilde{q}) \sin(2i). \quad (\text{A3})$$

This expression is compared to the N -body results in Fig. A1 for $\tilde{q} = 6$. The dependence on i is correctly predicted, but the amplitude is slightly overestimated (by about 10%). This is due in part to the N -body setup, where the eccentricity of the flyby is 1.1 rather than 1. This slight overestimate of the amplitude can lead to a larger discrepancy of the probability to generate $I_p > I_{p,\min}$, if this inclination threshold is close to $I_{\max}(\tilde{q})$. In fact, we can easily compute the theoretical probability assuming the flyby has a uniform distribution in $\cos i$:

$$\begin{aligned} p(I_p > I_{p,\min}) &= \frac{1}{2} \int_{I_p > I_{p,\min}} \sin(i) di \\ &= \int_{i < \frac{\pi}{2} - \frac{1}{2} \arcsin\left(\frac{I_{p,\min}}{I_{\max}(\tilde{q})}\right)}^{i > \frac{1}{2} \arcsin\left(\frac{I_{p,\min}}{I_{\max}(\tilde{q})}\right)} \sin(i) di \\ &= \cos\left[\frac{1}{2} \arcsin\left(\frac{I_{p,\min}}{I_{\max}(\tilde{q})}\right)\right] - \sin\left[\frac{1}{2} \arcsin\left(\frac{I_{p,\min}}{I_{\max}(\tilde{q})}\right)\right]. \end{aligned} \quad (\text{A4})$$

This probability is indicated by the dashed lines in Fig. 4.

This paper has been typeset from a \LaTeX file prepared by the author.